

Research Article

Application of Schwarz Christoffel Transformation as a Conformal Map in Solving Some Physical Problems

Ismaila Omeiza Ibrahim^{1*}, Manjak Nibron Haggai², Kwami Adamu Mohammed³

¹Dept. of Mathematics/Faculty of Physical Sciences, University of Maiduguri, Nigeria

^{2,3}Department of Mathematics, Abubakar Tafawa Balewa University Bauchi, Nigeria

*Corresponding Author: ibrahimismailaomeiza@gmail.com

Received: 21/Feb/2024; Accepted: 23/Mar/2024; Published: 30/Apr/2024

Abstract— This research work was purely on conformal mapping method. Existence of Schwarz-Christoffel transformation was briefly discussed and a lightning conductor was modelled as an illustration by the boundary-value problem in which the potential u is equal to zero at $x = 0$ which satisfies Laplace's equation in the half-space $x > 0$ and u to be bounded at infinity and the solution is bounded at $Z = \pm 1$. Another illustration which showed, the cross section of two metallic conductors the lower conductor is of infinite extent which lies on the real axis and at infinity. The other conductor is semi-infinite in length and extends from $-\infty + i$ to i . We also find the streamlines and equipotentials for this situation and obtained the voltage everywhere in space and we plot the equipotentials and electric flux lines, in which the charge tends to be concentrated at the edge of the upper plate. Furthermore, all the results were visualized with the aid of MATLAB, electric field is then directed downward, from the higher to the lower potential, and has magnitude equal to the voltage difference between the plates.

Keywords— conformal map, Schwarz-Christoffel transformation, Boundary value problem, laplace equation, stream lines, equipotentials, electric flux lines, lightning conductor.

1. Introduction

The Schwarz-Christoffel transformation is a mapping that maps a polygon to an the upper halfplane is termed Schwarz-Christoffel transformation. It is an integral that can be apply to elliptic integrals; the general case is usually considered unsolvable, since it cannot be expressed in terms of well-known functions. The advancement in computers that has made finite difference and finite element solutions possible can now be used to find the analytical solutions. A few centuries ago Analytical methods dominated in the solution of physical problems from the beginning of analysis. analytical functions were developed, resulting in numerous special functions due to a lot of researches. The Schwarz-Christoffel transformation was a popular analytic tool in fluid problems with polygon boundaries, in free streamline problems, and in plane elastic systems. Interest in the analytic solution of the Schwarz-Christoffel transformation stopped around 1960's, when analytical methods were overtaken by purely numerical methods in the solution of partial differential equations. Computer has also been used to handle analytical methods in what are called symbolic computer languages. Yet these still rely on classic well-known analytic functions. Since the 1970's, numerical methods have solved the Schwarz-Christoffel transformation successfully [8, 9]. Trefethen [10]

developed One of the best known and popular methods, particularly well explained, also discussed and advocated by Henrici [6]. That method is developed as a computer package, called SCPACK, which is freely available from its author. Variations and improvements of the numerical solution continue to appear [3, 5, 1, 2]. An improvement for elongated regions, using Trefethen's numerical integration, is given in Howell & Trefethen [7]. An application package with unlimited scope for MATLAB I is given in Driscoll [4]. The result is that the Schwarz-Christoffel transformation is used more frequently.

2. Experimental Method

We know that we can not prove Schwarz christoffel transformation without talking of its existence. Now, let us quickly see existence of Schwarz christoffel transformation.

2.1 EXISTENCE OF A MAPPING FUNCTION ON SCHWARZ-CHRISTOFFEL TRANSFORMATION

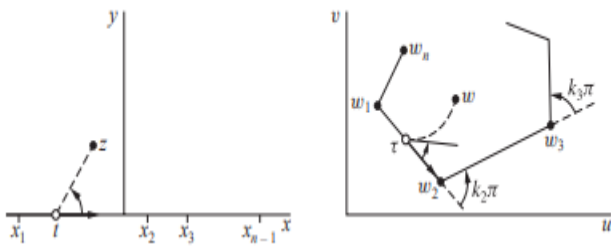


Fig. 1: Brown & Churchill [12]

From the proof of Wiam *et al.* [11]:

$$f'(z) = A(z - x_1)^{-k_1} (z - x_2)^{-k_2} \dots (z - x_{n-1})^{-k_{n-1}}$$

for the derivative of a function that is to map the real axis onto a polygon, let the factors

$(z - x_j)^{-k_j}$ ($j = 1, 2, \dots, n - 1$) represent branches of power functions with branch cuts extending below the real axis. To be specific, write

$$(z - x_j)^{-k_j} = \exp[-k_j \log(z - x_j)] = \exp[-k_j (\ln |z - x_j| + i\theta_j)]$$

and then

$$(z - x_j)^{-k_j} = |z - x_j|^{-k_j} \exp(-i k_j \theta_j) \quad \left(-\frac{\pi}{2} < \theta_j < \frac{3\pi}{2}\right)$$

where $\theta_j = \arg(z - x_j)$ and $j = 1, 2, \dots, n - 1$. This makes $f'(z)$ analytic everywhere in the half plane $y \geq 0$ except at the $n - 1$ branch points x_j . If z_0 is a point in that region of analyticity, denoted here by R , then the function

$$f(z) = \int_{z_0}^z f'(s) ds \tag{1}$$

is single-valued and analytic throughout the same region, where the path of integration from z_0 to z is any contour lying within R . Moreover, $F'(z) = f'(z)$

To define the function F at the point $z = x_1$ so that it is continuous there, we note that $(z - x_1)^{-k_1}$ is the only factor in expression that is not analytic at x_1 . Hence if $\varphi(z)$ denotes the product of the rest of the factors in that expression, $\varphi(z)$ is analytic at the point x_1 and is represented throughout an open disk $|z - x_1| < R_1$ by its Taylor series about x_1 . So we can write

$$f'(s) = (z - x_1)^{-k_1} \varphi(z) = (z - x_1)^{-k_1} \left[\varphi(x_1) + \frac{\varphi'(x_1)}{1!} (z - x_1) + \frac{\varphi''(x_1)}{2!} (z - x_1)^2 + \dots \right]$$

or

$$f'(z) = \varphi(x_1) (z - x_1)^{-k_1} + (z - x_1)^{1-k_1} \psi(z) \tag{2}$$

where ψ is analytic and therefore continuous throughout the entire open disk. Since $1 - k_1 > 0$, the last term on the right in equation (2) thus represents a continuous function of z throughout $y, the upper half of the disk, where $\text{Im } z \geq 0$, if we assign it the value zero at $z = x_1$. It follows that the integral$

$$\int_{z_1}^z (s - x_1)^{1-k_1} \varphi(s) ds$$

of that last term along a contour from z_1 to z , where z_1 and the contour lie in the half disk, is a continuous function of z at $z = x_1$. The integra

$$\int_{z_1}^z (s - x_1)^{-k_1} ds = \frac{1}{1-k_1} [(z - x_1)^{1-k_1} - (z_1 - x_1)^{1-k_1}]$$

along the same path also represents a continuous function of z at x_1 if we define the value of the integral there as its limit as z approaches x_1 in the half disk. The integral of the function along the stated path from z_1 to z is, then, continuous at $z = x_1$; and the same is true of integral (1) since it can be written as an integral along a contour in R from z_0 to z_1 plus the integral from z_1 to z . The above argument applies at each of the $n - 1$ points x_j to make F continuous throughout the region $y \geq 0$. From equation (1), we can show that for a sufficiently large positive number R , a positive constant M exists such that if $\text{Im } z \geq 0$, then

$$|f'(z)| < \frac{M}{|z|^{2-k_n}} \quad \text{whenever} \quad |z| > R \tag{3}$$

Since $2 - k_n > 1$, this order property of the integrand in equation (1) ensures the existence of the limit of the integral there as z tends to infinity; that is, a number w_n exists such that

$$\lim_{z \rightarrow \infty} F(z) = W_n \quad (\text{Im } z \geq 0), \tag{4}$$

Our mapping function, whose derivative is given by equation (1), can be written

$f(z) = F(z) + B$, where B is a complex constant. The resulting transformation,

$$w = A \int_{z_1}^z (s - x_1)^{-k_1} (s - x_2)^{-k_2} \dots (s - x_{n-1})^{-k_{n-1}} ds + B \tag{5}$$

is the Schwarz-Christoffel transformation, named in honor of the two German mathematicians H. A. Schwarz (1843–1921) and E. B. Christoffel (1829–1900) who discovered it independently. Transformation (5) is continuous throughout the half plane $y \geq 0$ and is conformal there except for the points x_j . We have assumed that the numbers k_j satisfy conditions (3). In addition, we suppose that the constants x_j and k_j are such that the sides of the polygon do not cross, so that the polygon is a simple closed contour. Then, as the point z describes the x axis in the positive direction, its image w describes the polygon P in the positive sense; and there is a one to one correspondence between points on that axis and points on P . According to condition (4), the image w_n of the point $z = \infty$ exists and $w_n = W_n + B$.

If z is an interior point of the upper half plane $y \geq 0$ and x_0 is any point on the x axis other than one of the x_j , then the angle from the vector t at x_0 up to the line segment joining x_0 and z is positive and less than π (Fig. 1). At the image w_0 of x_0 , the corresponding angle from the vector τ to the image of the line segment joining x_0 and z has that same value. Thus, the images of interior points in the half plane lie to the left of the sides of the polygon, taken counterclockwise.

Given a specific polygon P, let us examine the number of constants in the Schwarz–Christoffel transformation that must be determined in order to map the x axis onto P. For this purpose, we may write $z_0 = 0$, $A = 1$, and $B = 0$ and simply require that the x axis be mapped onto some polygon P' similar to P. The size and position of P' can then be adjusted to match those of P by introducing the appropriate constants A and B.

The numbers k_j are all determined from the exterior angles at the vertices of P. The $n - 1$ constants x_j remain to be chosen. The image of the x axis is some polygon P' that has the same angles as P. But if P' is to be similar to P, then $n - 2$ connected sides must have a common ratio to the corresponding sides of P; this condition is expressed by means of $n - 3$ equations in the $n - 1$ real unknowns x_j . Thus two of the numbers x_j , or two relations between them, can be chosen arbitrarily, provided those $n - 3$ equations in the remaining $n - 3$ unknowns have real-valued solutions.

When a finite point $z = x_n$ on the x axis, instead of the point at infinity, represents the point whose image is the vertex w_n , it follows that the Schwarz–Christoffel transformation takes the form:

$$w = A \int_{z_1}^z (s - x_1)^{-k_1} (s - x_2)^{-k_2} \dots (s - x_{n-1})^{-k_{n-1}} ds \quad (6)$$

where $k_1 + k_2 + \dots + k_n = 2$. The exponents k_j are determined from the exterior angles of the polygon. But, in this case, there are n real constants x_j that must satisfy the $n - 3$ equations noted above. Thus three of the numbers x_j , or three conditions on those n numbers, can be chosen arbitrarily when transformation (6) is used to map the x axis onto a given polygon.

3. Results and Discussion

In what follows we now consider some illustrations to appreciate the use of Schwarz Christoffel Transformation in practice.

Illustration 1

A lightning conductor is modelled by the boundary-value problem illustrated in Figure 2. The potential u is equal to zero at $x = 0$ and satisfies Laplace’s equation in the half-space $x > 0$, except on the line $y = 0, x > 1$, where $u = 1$. We also require u to be bounded at infinity.

Solution.

The domain D is the image of the strip $0 < X < \pi/2, -\infty < Y < \infty$ under the map $z = \sin Z$. In the Z-plane we have $\nabla^2 U = 0$ with $U = 0$ at $X = 0$ and $U = 1$ at $X = \pi/2$, as shown in Figure 41. The solution in the Z-plane is $U = \text{Re} W = \text{Re}(2Z/\pi)$, and therefore

$$u = \frac{2}{\pi} \text{Re}(\sin^{-1} z) \quad (7)$$

$$\Rightarrow \frac{d}{dz} \left(\frac{2}{\pi} \sin^{-1} z \right) = \frac{2}{\pi} \frac{1}{\sqrt{1 - z^2}} \quad (8)$$

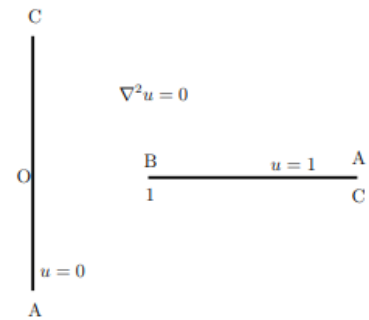


Figure 2: A model for a lightning conductor.

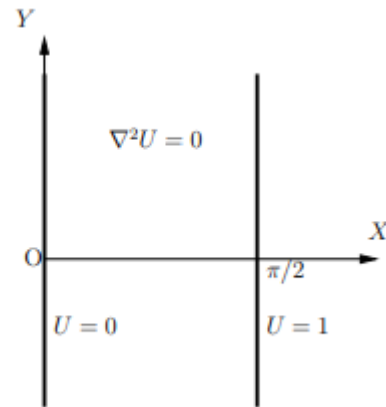


Figure 3: The problem from Figure 2 transformed by the map $Z = \sin^{-1} z$

And it follows that $|\nabla u| \rightarrow \infty$ as $z \rightarrow 1$, at the tip of the spike.

This example could also have solved by using Schwarz-Christoffel mapping to map the upper half Z-plane to D. The vertices marked A, B, C in figure 2 have the exterior angles

$$\beta_A = \frac{3}{2}, \quad \beta_B = -1, \quad \beta_C = \frac{3}{2} \quad (9)$$

we can choose to map

$$Z = -1 \text{ to } A, \quad Z = 0 \text{ to } B, \quad Z = 1 \text{ to } C, \quad (10)$$

and because of symmetry, we are also free to map

$Z = \infty$ to $z = 0$. Then the Schwarz-Christoffel formula gives

$$z = \frac{1}{\sqrt{1 - z^2}} \quad (11)$$

The problem in the Z-plane is shown in figure 42. The solution bounded at $Z = \pm 1$ is simply

$$U = \frac{1}{\pi} (\arg(Z + 1) - \arg(Z - 1)) = \text{Im} \left[\frac{1}{\pi} \log \left(\frac{Z - 1}{Z + 1} \right) \right] \quad (12)$$

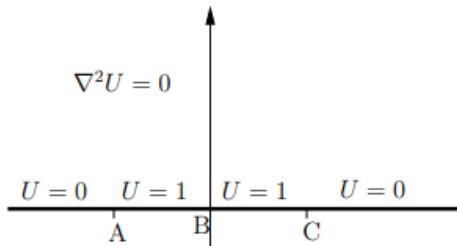


Figure 4: The problem from Figure 40 transformed by the map $z = 1/\sqrt{1 - Z^2}$

and by inverting the conformal map we find

$$u = \frac{1}{\pi} \text{Im} \left[\log \left(\frac{\sqrt{z^2 - 1} - z}{\sqrt{z^2 - 1} + z} \right) \right]$$

which is equivalent to (7).

Illustration 2

Imagine that the above shows the cross section of two metallic conductors. The lower conductor is of infinite extent, lies along $y = 0$ and goes from $x = -\infty$ to $x = \infty$. The other conductor is semi-infinite in length and extends from $x = -\infty + i$ to $x = i$. The second conductor is 1 unit above the first and is maintained at a potential of 1 volt while the lower one is at ground (zero) potential. Our problem is to find the streamlines and equipotentials for this situation and find the voltage everywhere in space. We will apply the Schwarz-Christoffel transformation to the configuration shown below in Figure 43b and then let the angle α tend to zero to achieve the configuration shown above which will be mapped onto the real axis in the w plane with the exterior of the above figure mapped into the upper half of the w plane.

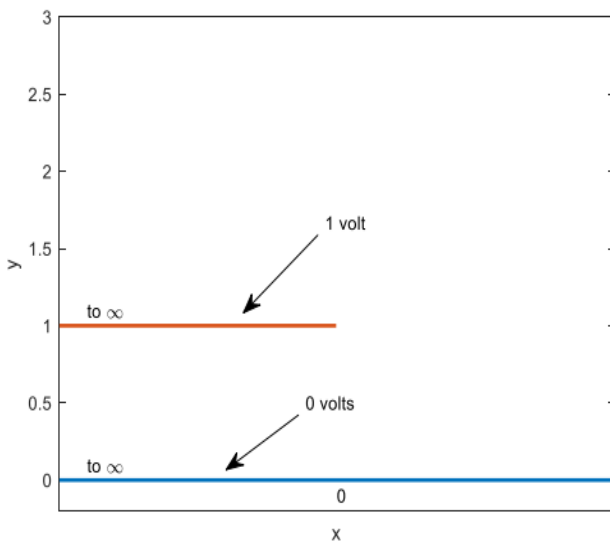


Figure 5 a

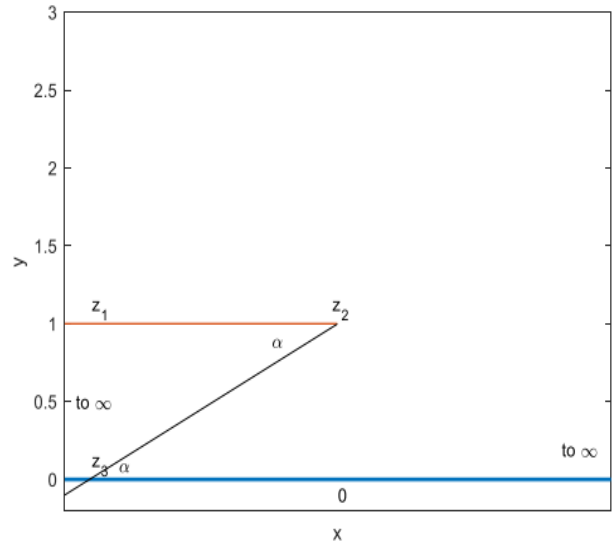


Figure 5 b

Following the notation of figure 1 we have that $\alpha_2 = 2\pi - \alpha$ and $\alpha_3 = \alpha$. The point $z_2 = i$ will get mapped into $w_2 = -1$ and z_3 will get mapped into $w_3 = 0$. Notice that z_1 , which is at infinity, will map into $w_1 = \infty$. We can explain that z_1 and z_3 which both lie at infinity get mapped into different locations in the w -plane. We imagine that z_1 and z_2 lie on different sides of a branch cut of $z = F(w)$ where $F(w)$ is the right side of eq. (6). notice for example that the function $w = e^{-\pi z}$ evaluated along the lines $z = x$ and $x + i$ have different limits as $x \rightarrow -\infty$ and they differ in sign. In this case, the inverse transformation is $z(w) = \frac{-1}{\pi} \text{Log} w$ which has a branch cut. The above configuration in the figure is to be mapped into that shown in Figure 6 below. Notice too, for the above figure, that we have moved along the polygon (from z_1 to z_2 etc.) in such a way that the region above and outside the above broken line, which is to be mapped into the upper half of the w plane is on our left. We thus have from Eq.(6) .

$$z(w) = A \int (w + 1)^{-k_1} (w)^{-k_2} dw + B$$

Passing to the limit $\alpha \rightarrow 0$ we have

$$z(w) = A \int (w + 1)(w)^{-1} dw + B = Aw + A \text{Log} w + B \quad (14)$$

If we take the lower limit as -1 and $B = i$, then we have that $w_2 = -1$ has image $z_2 = i$ as required. The integration is easy and we have

$$\begin{aligned} z &= A \text{Log} w + Aw - A \text{Log}(-1) + A + i \\ &= A \text{Log} w + Aw - A i \pi + A + i \\ &= A \text{Log} w + A(w - i \pi + 1) + i \end{aligned}$$

Suppose we move the negative real axis in the w -plane toward $w = 0^-$. We are approaching $w = 0$ (which is w_3 , see figure below) from the

left. Due to the logarithm, if A were complex then the imaginary part of this expression would become unbounded as $u \rightarrow 0^-$. But we want the imaginary part to be bounded, as we see from figure 43. Thus, A is real.

The Schwarz Christoffel transformation maps the domain exterior to the broken line in the above figure into the upper half of the w plane with the boundary in the figure mapped into the real axis in the w plane. If that is the case, in the present problem, as we proceed along the line $Im(w) = 0, 0 < Re(w) < \infty$ using the transformation $z(w)$ the image points in the z-plane must lie on the line $Im(z) = 0$. Since A is known to be real, the expression $z = A \text{Log} w + A(w - i\pi + 1) + i$, where w is positive real and is real if $A = \frac{1}{\pi}$. Thus finally:

$$z(w) = \frac{1}{\pi} (w + \text{Log} w + 1) \tag{15}$$

There is no way to solve for w as a function of z. However, as before in this situation, we can plot the equipotentials and electric flux lines. Note that the configuration of Figures 5 a and b, is mapped, in the limit, by Eq.(15) into the w plane as show below.

Table 1.

Plates (w)	Values	Volts
1	∞	1
2	-1	1
3	0	1
4	1	0
5	2	0
.	.	.
.	.	.
50	47	0

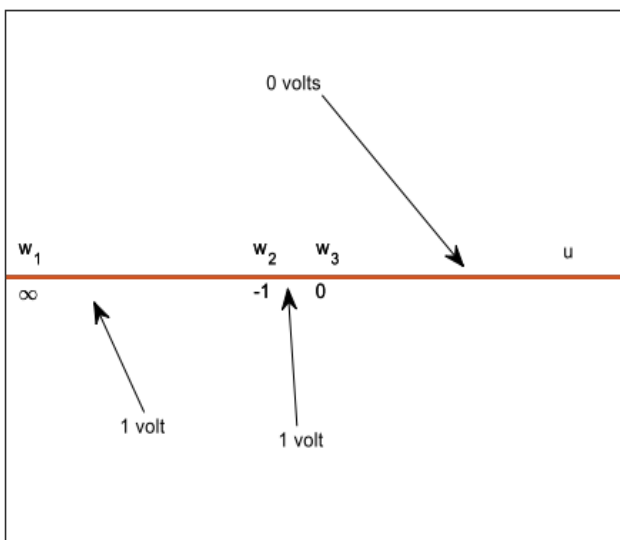


Figure 6

Observe that potential $\phi(u, v)$ on the line $Im(w) = v = 0$ is given by $\phi(u, 0) = 1$ for $-\infty < u < 0$ and $\phi(u, 0) = 0$ for $0 < u < \infty$. We can find the potential in the upper half space from the poisson integral formula as well $\phi(u, v) = \frac{1}{\pi} \tan^{-1} \left(\frac{v}{u} \right)$. The \tan^{-1} is interpreted as the imaginary part of $\text{Log} w$ (the principal branch). In this way we obtained $0 \leq \phi(u, v) \leq 1$ in the upper half of the w-plane.

Thus, it should be apparent that the complex potential in the w-plane is $\Phi(u, v) = \phi(u, v) + i\psi(u, v) = \frac{-i}{\pi} \text{Log} w$

$$= \frac{1}{\pi} \tan^{-1} \left(\frac{v}{u} \right) + \frac{-i}{\pi} \text{Log} \sqrt{u^2 + v^2} \tag{16}$$

The equipotentials in the w-plane are lying on the surfaces for which $V_0 = \frac{1}{\pi} \tan^{-1} \left(\frac{v}{u} \right)$ so that $v = u \tan(\pi V_0)$ $0 \leq V_0 \leq 1$

These are of course straight lines(rays) leaving the origin in the upper half of the $w = u + iv$ plane.

Note that as $V_0 \rightarrow 1/2$ we have $u \rightarrow 0$ for any finite v. On the equipotentials we have

$$w = u + iu \tan(\pi V_0) \tag{18}$$

We can substitute this expression into Eq.(15) to find the image of each equipotential in the z plane. We must be careful to use this expression in such a way that $Im w \geq 0$ because it is this region that forms the image of the domain whose boundary is shown in Figures 5 (a)and(b).

Thus, if $0 \leq V_0 \leq 1/2$ we have that $0 \leq \tan(\pi V_0)$ and in using Eq. (152) we are restricted to $u \geq 0$. Conversely, if $1/2 \leq V_0 \leq 1$ we have $\tan(\pi V_0) < 0$ and we are restricted to $u \leq 0$.

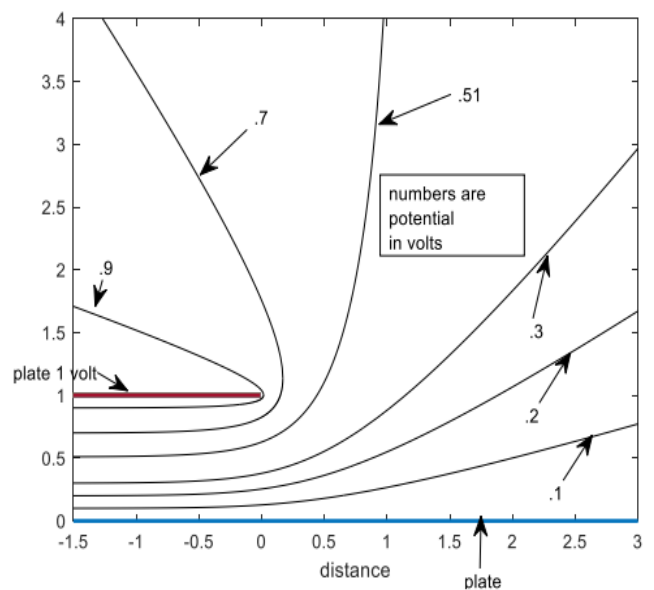


Figure 7

The streamlines for the above configuration are at each point tangent to the electric field and electric flux density vector. The streamlines are the lines along which the stream function $\psi(x, y)$ assumes constant values. For the present problem we have from Eq.(18) that the stream function in the w plane is

$$\psi(u, v) = \frac{-1}{\pi} \text{Log} \sqrt{u^2 + v^2} \tag{19}$$

We can set this equal to a number of real values and plot the locus in the z plane for each value. By using uniformly spaced values of ψ we can see how tightly or sparsely spaced these loci are in the z plane. The more tightly spaced they are at the boundaries (the plates in the above figures) the higher the concentration of charge. The charge is positive at each point on the plate at the

higher potential, $y = 1, x < 0$ and negative at the plate of lower potential $y = 0, -\infty < x < \infty$. Let γ be a value of $\psi(u, v)$. We have Eq.(19) that

$u^2 + v^2 = e^{-2\pi\gamma}$. These are circles of radius $e^{-\pi\gamma}$, centered at the origin in the w-plane. These circles are valid only in the space $v \geq 0$. We now map circles, corresponding to uniformly spaced values of

$\gamma = \psi$. The radii of the circles are not uniformly spaced because they are equal to $e^{-\pi\gamma}$ which is not a linear function. The mapping is made from w-plane into the z-plane so as to produce the streamlines (flux lines) for the above figure. Notice this expression $z(w) = \frac{1}{\pi} (w + \text{Log} w + 1)$. If we wish to obtain values

of z for the region between plates, which is where $\text{Re}(z) < 0, 0 < \text{Im}(z) < 1$, we will require that, $0 \leq \text{arg}(w) + \text{Im}(w) < \pi$. Also a necessary but not sufficient condition is that $0 < \text{Re}(w) \leq 1$ as can be seen from study of Eq.(15) from the resulting plot

we have taken the increments of ψ as $\frac{1}{15}$. The reader might wish to experiment with other values.

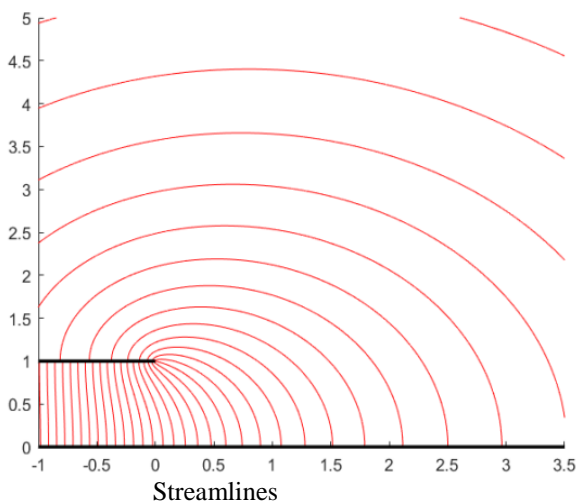


Figure 8 We see that charge tends to be concentrated at the edge of the upper plate. As we move to the left, between the plates, the

field becomes uniform and has the behavior appropriate to an infinite parallel plate capacitor with no fringe field. The electric field is then directed downward, from the higher to the lower potential, and has a magnitude equal to the voltage difference between the plates divided by their separation, i.e. 1. The field as a vector is simply $-i$.

Ofcourse we can obtain electric field at any point of interest.

Since, electric field $E = -\left(\frac{d\Phi}{dz}\right)$. We have

also that $\frac{d\Phi}{dz} = \frac{d\Phi}{dw} \frac{dw}{dz} = \frac{d\Phi}{dz} \div \frac{dz}{dw}$ thus, using Eq.(15)

and (16) we have

$$E(w) = \frac{-iw}{|w|^2 + w} \tag{20}$$

For every value of z of interest, we must find the corresponding value of w by using Eq. (15)

Notice that at $-0.5 + 0.5i$, which is between the plates, the electric field is downward directed with a magnitude of roughly 1 and points very slightly to the right

(as predicted by Fig. 46). At $0.5 + 0.5i$, which is not between the plates, and is referred to as the region of “fringe field”, the field has weakened in the downward direction from the previous value and shows fringing toward the right, while at the third location

we are close to the upper edge where the field is quite strong, points downward but has an even stronger component toward the right. Of

the three values of electric field we have considered the third is strongest owing to the singularity in field strength at the point $z = i$.

3.1 Results Discussion

Schwarz-Christoffel Transformation was efficiently used as a conformal map on physical system. Which was later illustrated as shown above and was visualized with the aid of MATLAB. Illustration 1 shows how a lightning conductor is modelled by the boundary-value problem illustrated in Figure 2. The potential u is equal to zero at $x = 0$ and satisfies Laplace’s equation in the half-space $x > 0$, except on the line $y = 0, x > 1$, where $u = 1$. We also showed that u to be bounded at infinity. Furthermore, The problem in the Z-plane is shown in figure 4. The solution bounded at $Z = \pm 1$ is simply shown in equation (12) and by inverting the conformal map we obtained

$$u = \frac{1}{\pi} \text{Im} \left[\log \left(\frac{\sqrt{z^2 - 1} - z}{\sqrt{z^2 - 1} + z} \right) \right] \text{ which is equivalent to (7).}$$

Illustration 2 shows the cross section of two metallic conductors as shown in figure 5a. The lower conductor is of infinite extent, lies along $y = 0$ and goes from $-\infty$ to $x = \infty$. The other conductor is semi-infinite in length and extends from $-\infty + i$ to i . The second conductor is 1 unit above the first and is maintained at a potential of 1 volt while the lower one is at ground (zero) potential. In which our problem is to find the streamlines and equipotentials for this situation and find the voltage everywhere in space. We then apply the Schwarz-Christoffel transformation to the configuration shown below in Figure 5b

and then let the angle α tend to zero to achieve the configuration shown above which will be mapped onto the real axis in the w plane with the exterior of the above figure mapped into the upper half of the w plane. We were able to plot the equipotentials and electric flux lines as shown in figure 7. We see that the charge tends to be concentrated at the edge of the upper plate. As we move to the left, between the plates, the field becomes uniform and has the behavior appropriate to an infinite parallel plate capacitor with no fringe field. The electric field is then directed downward, from the higher to the lower potential, and has a magnitude equal to the voltage difference between the plates divided by their separation, i.e. The field as a vector is simply $-\hat{i}$ as shown in figure 8.

4. Conclusion and Future Scope

Our work was based purely on conformal mapping method. This study dealt with the application of Schwarz christoffel transformation on physical system which is an extension of wiam et al [11] and Calixto et. al, [13] respectively. Thus, the following recommendations are hereby presented :

[1] Since the study dealt with application on physical system an attempt should be made in applying Swartz Christoffel Transformation in other sectors of the economy such as in transport and finance.

[2] It is recommended that, numerical techniques should be used in the study of conformal maps on physical system.

Data Availability (Size 10 Bold)

Our data was collected and collated based on our existing literatures.

Conflict of Interest

All authors contributed in this research and there is no conflict of interest.

Funding Source

This research was from a personal funding.

Authors' Contributions

Ibrahim help in drafting, Manjak works on existence and methodology . Kwami , manjak and Ibrahim presented the results . while all the authors works on result discussion and conclusion..

Acknowledgements

The authors wish to acknowledge all the references and the reviewer for their contributions which helps to improve the quality of the work.

References

[1] M.A. Chaudhry, R. Schinzinger, 'Numerical computation of the Schwarz-Christoffel transformation parameters for conformal mapping of arbitrarily shaped polygons with finite vertices', *COMPEL*, The International Journal for Computation and Mathematics in Electrical and Electronic Engineering volume 2 Issue 1, pp. 263-275, 1992.

- [2] J.M. Chuang, Q.Y. Gui, C.C. Hsiung, 'Numerical computation of Schwarz-Christoffel transformation for simply connected unbounded domain', *Computer Methods in Applied Mechanics and Engineering* Volume 10, Issue 5, pp. 93-109, 1993.
- [3] E. Costamagna, 'On the numerical inversion of the Schwarz-Christoffel conformal transformation', *IEEE Transactions on Microwave Theory and Techniques* MTT Volume 35, Issue 1, pp. 35-40, 1987.
- [4] T.A. Driscoll, 'Algorithm 756: A MATLAB toolbox for Schwarz-Christoffel mapping', *ACM Transactions on Mathematical Software* Volume 22, Issue 2, pp. 168-186, 1996.
- [5] A. Gilicz, 'Alternative, useful conformal mapping method can be used for odd-shaped fields', *Oil & Gas Journal* Volume 85, Issue 23, pp. 57- 62, 1987.
- [6] P. Henrici, 'Applied and computational complex Analysis', *Pure and Applied Mathematics. John Wiley & Sons*, New York, NY, USA. Vol. 3, 1986.
- [7] L.H. Howell, L.N. Trefethen, 'A modified Schwarz-Christoffel transformation for elongated regions', *SIAM g. Sci. Stat. Coraput.* Volume 11, Issue 5, pp. 928-949, 1990.
- [8] D. Howell, 'The application of numerical methods to the conformal transformation of polygonal boundaries', *J. Inst. Maths. Applics.* Volume 12, Issue 1 pp. 125-136, 1973.
- [9] W. Squire, 'Computer implementation of the Schwarz-Christoffel transformation', *Journal of the Franklin Institute* Volume 299, Issue 5, pp. 315-322, 1975.
- [10] L.N. Trefethen, 'Numerical computation of the Schwarz-Christoffel transformation', *SIAM J. Sei. Star. Comput.* Volume 1, Issue 1, pp. 82-102, 1980.
- [11] A. A Wiam, , I.E Omar, A. K Zaynab, A.A Abdusalam, 'Conformal mapping as a tool in solving some mathematical and physical problems' *European Academic Research.* Volume 3. Issue 10, pp. 1-19, 2021
- [12] R. V Churchill, J.W Brown, 'Complex variables and Applications' *MC Grawn – Hill.* Eight Edition, Volume 1, Issue 2 pp. 373-395, 2009.
- [13] W. P. Calixto, B. Alvarenga, J. C. da Mota, Brito, C. da, M. Wu, A. J. Alves, C. F. Antunes, ' Electromagnetic Problems Solving by Conformal Mapping: A Mathematical Operator for Optimization'. *Journal of Mathematical Problems in Engineering*, Volume 1, Issue 1 pp. 1-19, 2010.

AUTHORS PROFILE

Ibrahim Ismaila Omeiza earned his B.Sc., M. Sc., and Ph.D.(in view) in mathematics from Kogi State University Ayingba in 2012, M. Sc University of Maiduguri in 2018, and currently undergoing his Ph.D in ATBU Bauchi since 2021 till date, respectively. He is currently working as a Lecturer in Department of mathemaics IN UNIMAID, Maiduguri since 2020. He is a member of NMS since 2018, Life member of ASUU since 2020 and a life member of the TRCN Research Spectrum since 2015. He has published more than 10 research papers in reputed international journals including *Analele Universității Din Oradea* and conferences including *Turkish Journal of Inequalities* and it's also available online. His main research work focuses on Conformal mapping, Geometric function theory, Numerical Analysis and Complex Analysis. He has 8 years of teaching experience and 4 years of research experience.

Manjak Nibron Haggai earned his B. Sc., M. Tech., and Ph.D. in mathematics from UNIJOS, Jos in 1990, 1996, and 2006, respectively. He is currently working as Professor in Department of mathemaics from ATBU, Bauchi since 2013. He is a member of NMS since 2010, Life member of ASUU since 1991 and a life member of the NUC Research Spectrum

since 2015. He has published more than 48 research papers in reputed international journals which are available online. His main research work focuses on Conformal mapping, Topology, functional analysis, optimization theory and Numerical Analysis. He has 33 years of teaching experience and 29 years of research experience.

Kwami Adamu Mohammed earned his B. Sc., M. Tech., and Ph.D. in mathematics from ATBU, Bauchi in 1990, 1998, and 2012, respectively. He is currently working as Professor in Department of mathematics from ATBU, Bauchi since 2021. He is a member of NMS since 2010, Life member of ASUU since 1991 and a life member of the NUC Research Spectrum since 2015. He has published more than 36 research papers in reputed international journals are available online. His main research work focuses on Fluid Mechanics, optimization theory and Numerical Analysis. He has 29 years of teaching experience and 22 years of research experience.
